

Supporting Information

Fluorinated Paclitaxel Prodrugs for Potentiated Stability and Chemotherapy

Bowen Jiang,^{a,b} Dengyuan Hao,^{a,b} Chaonan Li,^{a,b} Shaojin Lu,^{a,b} Qing Pei^{a,*} and Zhigang Xie^{a,b,*}

^a State Key Laboratory of Polymer Physics and Chemistry, Changchun Institute of Applied Chemistry, Chinese Academy of Sciences, Changchun, Jilin 130022, P. R. China

^b University of Science and Technology of China, Hefei, Anhui 230026, P. R. China

***Corresponding author:**

E-mail address: peiqing@ciac.ac.cn, xiez@ciac.ac.cn.

Contents:

EXPERIMENTAL SECTION

SUPPLEMENTARY FIGURES

Fig. S1. The synthetic route of disulfide bond-bridged fluorinated/alkylated PTX prodrugs. i, EDC·HCl and DMAP at 25 °C.

Fig. S2. The synthetic route of dicarbide bond-bridged fluorinated PTX prodrug PC-17F. i, DMAP and pyridine at 25 °C; ii, EDC·HCl and DMAP at 25 °C.

Fig. S3. The synthetic route of BDP-17F. i, EDC·HCl and DMAP at 25 °C.

Fig. S4. ¹H NMR spectrum of PTX-SS-COOH in CDCl₃.

Fig. S5. ¹H NMR spectrum of PS-17F in CDCl₃.

Fig. S6. ¹H NMR spectrum of PS-9F in CDCl₃.

Fig. S7. ¹H NMR spectrum of PS-3F in CDCl₃.

Fig. S8. ¹H NMR spectrum of PS-CH in CDCl₃.

Fig. S9. ¹H NMR spectrum of PC-17F in CDCl₃.

Fig. S10. ¹H NMR spectrum of BDP-17F in CDCl₃.

Fig. S11. ESI-TOF mass spectrum of PS-17F.

Fig. S12. ESI-TOF mass spectrum of PS-9F.

Fig. S13. ESI-TOF mass spectrum of PS-3F.

Fig. S14. ESI-TOF mass spectrum of PS-CH.

Fig. S15. ESI-TOF mass spectrum of PC-17F.

Fig. S16. ESI-TOF mass spectrum of BDP-17F.

Fig. S17. The critical aggregation concentration (CAC) of PS-17F (a), PS-9F (b) and PS-CH (c).

Fig. S18. The size distribution and picture of PS-9F NPs at the concentration of 0.34 mg mL⁻¹.

Fig. S19. The size of PS-17F NPs, PS-9F NPs, PS-CH NPs and PC-17F NPs after storage in water for 20 days.

Fig. S20. The redox-responsive PTX release from PC-17F NPs upon being treated with

10 mM DTT (a) and 10 mM H₂O₂ (b).

Fig. S21. UV-vis absorption spectra (a) and FL emission spectra (b) of BDP-OH and BDP-17F at equivalent BDP concentration of 2 μM in DMF.

Fig. S22. ζ-potential of 17F co-NPs and PS-17F NPs.

Fig. S23. Tumor accumulation of PS-17F NPs and PS-CH NPs (n = 3). *P < 0.05, **P < 0.01, and ***P < 0.001.

EXPERIMENTAL SECTION

Materials. Paclitaxel (PTX) was purchased from Dalian Meilun Biotechnology Co., Ltd.. 4-dimethylaminopyridine (DMAP, Aladdin) was used as received. 1-Ethyl-3-(3-dimethylaminopropyl) carbodiimide hydrochloride (EDC·HCl) was purchased from Shanghai yuanye Bio-Technology Co., Ltd.. 2,2'-disulfanediyldiacetic acid was purchased from TCI Shanghai Co., Ltd.. 1H,1H,2H,2H-perfluoro-1-decanol and 1-tetradecanol were purchased from Tianjin Heowns Biochemical Technology Co., Ltd.. 3,3,3-trifluoro-1-propanol and 1,1,2,2-tetrahydroperfluoro-1-hexanol were purchased from Energy Chemical Co., Ltd.. Chloroform-d (CDCl₃) was purchased from Qingdao Tenglong Weibo Technology Co., Ltd.. Ultrapure water was prepared from a Milli-Q system (Millipore, USA). Annexin V-FITC/PI apoptosis detection kit was obtained from Jiangsu KeyGEN Biotechnology Co., Ltd.. The other chemicals were used as obtained commercially.

Characterization. Analytical balance (XS105DU) and Rainin Pipettes from METTLER TOLEDO were used to quantify solid and liquid respectively. The morphology of the nanoparticles was determined by JEOL JEM-1011 electron microscope with acceleration voltage of 100 kV. Size distribution and ζ -potential of the nanoparticles were characterized by Malvern Zeta-sizer Nano. CLSM images were obtained from a Zeiss LSM 700 (Zurich, Switzerland).

The critical aggregation concentration (CAC) of the prodrugs. The CAC of the prodrugs were investigated by Nile Red as fluorescent probe. In brief, 1mL PS-17F NPs, PS-9F NPs or PS-CH NPs at different concentration were stirred intensely with 0.16 μ g Nile Red overnight, then the fluorescence intensity was detected by fluorescence spectrophotometer.

In vitro stability of NPs. To investigate in vitro stability, the prodrug NPs were cultured with solution containing 5% glucose, PBS (pH 7.4) solution containing 10% FBS or DMEM at 37 °C for different time. The changes of particle size were measured by DLS.

Cell lines and cell culture. HeLa (human cervical carcinoma), 4T1 (mouse breast cancer) cell lines were cultured in Dulbecco's modified Eagle's medium (DMEM, GIBCO) with 10% (v/v) heat-inactivated FBS (GIBCO). Cells were cultured in a humidified incubator at 37 °C with 5% CO₂, and the culture medium was replaced once every day.

Cellular uptake measured by CLSM and FCM. The cellular uptake of 17F co-NPs was evaluated by confocal laser scanning microscope (CLSM). First, HeLa cells were seeded in six-well culture plates (2×10^5 cells per well) and allowed to adhere for 24 h. Then, the original medium was removed and replaced by 17F co-NPs diluted with fresh culture medium to the concentration of BDP-17F at 0.5 μ M and incubated for additional 0.5, 2 and 4 h at 37 °C. After being stained by hoechst 33258 for 5 min to track cells nuclei, the samples were imaged by CLSM. For *in vitro* quantified endocytosis, the resuspended cell pellets harvested by centrifugation after being incubated with

corresponding co-NPs at the concentration of BDP-17F at 1 μ M for different time at 37 $^{\circ}$ C and 4 $^{\circ}$ C were examined by FCM.

Cell viability assays. The cytotoxicity of Taxol and the prodrug NPs against HeLa cells was examined via an MTT assay. In short, HeLa cells were seeded in 96-well plates at a density of 2×10^3 cells per well with 100 μ L DMEM. After adhering overnight, the incubation media was discarded and replaced with Taxol and PTX prodrug NPs diluted with the fresh media to desired concentrations and incubated for another 48 h. Then, 20 μ L of MTT (5 mg/mL, PBS) was added and the cells were incubated at 37 $^{\circ}$ C for additional 4 h. Then, the culture medium supernatant was carefully removed and 150 μ L of dimethyl sulfoxide (DMSO) was added to each well to dissolve the formed violet formazan crystals. Ultimately, the plates were shaken for 3 min, and the absorbance of violet product was determined at 490 nm by a microplate reader.

Calcein-AM/PI staining tests. To further investigate the antitumor efficacy of prodrug NPs, HeLa cells were co-stained with the calcein-AM and propidium iodide (PI) to differentiate dead (red) and live (green) cells. Briefly, after incubating HeLa cells with PBS, Taxol, PS-17F NPs, PS-9F NPs, PS-CH NPs and PC-17F NPs at equivalent PTX concentration of 10 μ M for 24 h, the incubation medium was removed and calcein-AM/PI was added to stain cells for another 30 min at ambient temperature. Finally, the treated cells were imaged by fluorescence microscopy.

Cell apoptosis and necrosis detection assays. The cell early and late apoptosis induced by chemotherapy of the prodrug NPs were quantified by FCM. Briefly, HeLa cells were cultured with PBS and Taxol, PS-17F NPs, PS-9F NPs, PS-CH NPs and PC-17F NPs at equivalent PTX concentration of 10 μ M for 24 h, and then cells were washed, harvested and collected, and stained with Annexin V-FITC and PI for about 20 min. Finally, the cell apoptosis and necrosis ratios were quantified by FCM.

Visualization of microtubule networks via the immunofluorescent staining assays. The immunostaining assays of tubulin were used to identify the suppress effect of prodrug NPs. In simple terms, HeLa cells were incubated with PBS, Taxol, PS-17F NPs, PS-9F NPs, PS-CH NPs and PC-17F NPs at equivalent PTX concentration of 10 μ M for 24 h. After that, the medium supernatant was removed and cells were washed gently, fixed with 4% paraformaldehyde (1 mL well⁻¹) for about 12 min and washed 2 times with PBS (pH 7.4) solution containing 0.1% Triton X-100. Then cells were incubated with immunostaining second antibody of tubulin diluted by PBS (pH 7.4) solution containing 0.1% Triton X-100 and 3% BSA for 30 min at room temperature in dark. Subsequently, the stained cells were imaged by CLSM.

Animal studies. All animal experiments have been approved by the Animal Welfare and Ethics Committee of Changchun Institute of Applied Chemistry, Chinese Academy of Sciences, and carried out according to the NIH guidelines for the care and use of laboratory animals (NIH publication No. 85-23 Rev. 1985). Female balb/c mice were obtained and raised under required conditions. The *in vivo* tumor accumulation of PS-17F NPs and PS-CH NPs were assessed using 4T1 tumor-burdened mice. When the tumor volume reached approximately 500 mm³, PS-17F NPs and PS-CH NPs were

injected intravenously at equivalent PTX dose of 15 mg/kg (drug weight/body weight) to the mice (n=3). At 6 h-post injection, the mice were sacrificed, and their tumor and liver were harvested, weighed and homogenized in PBS (1 g tissues/10 mL PBS). Then, the samples were centrifuged at 5000 r/min, and the supernatants were collected and extracted with methyl tertiary butyl ether for three times. The samples were left overnight to volatilize methyl tertiary butyl ether, and then 0.2 mL methanol was added. The tissue concentration of PTX and prodrugs was measured by HPLC with UV-vis detection wavelength at 231 nm. Mice with subcutaneous 4T1 xenografts tumor were utilized as animal modal to evaluate antitumor effects. 4T1 cells were subcutaneously inoculated into the lateral aspect of the anterior right limb of mice (3×10^6 cells in 0.1 mL PBS). The tumor-bearing mice were randomly divided into four groups (n = 5): (1) normal saline (blank control), (2) Taxol, (3) PS-17F NPs and (4) PS-CH NPs groups. Before treatment, mice were marked, weighed and measured. Then PBS, Taxol, PS-17F NPs and PS-CH NPs were intravenously injected into the corresponding tumor-bearing mice at equivalent PTX dose of 15 mg/kg (drug weight/body weight), respectively, for 4 times every other day. At designed time (0, 2, 4, 6, 8, 10, 12, 14 and 16 d), the body weight of mice and tumor volume were measured. At day 16, mice were sacrificed, and tumor was excised to intuitively evaluate the tumor inhibition. In order to investigate the safety of formulations, the potential hepatic and renal toxicity and blood routine were examined. Main organs (heart, liver, spleen, lung and kidney) and tumor were collected, fixed in 4% paraformaldehyde solution, and then embedded in paraffin, sliced and stained with hematoxylin and eosin (H&E) to evaluate potential toxicity for main organs and apoptosis degrees for cancer cells.

SUPPLEMENTARY FIGURES

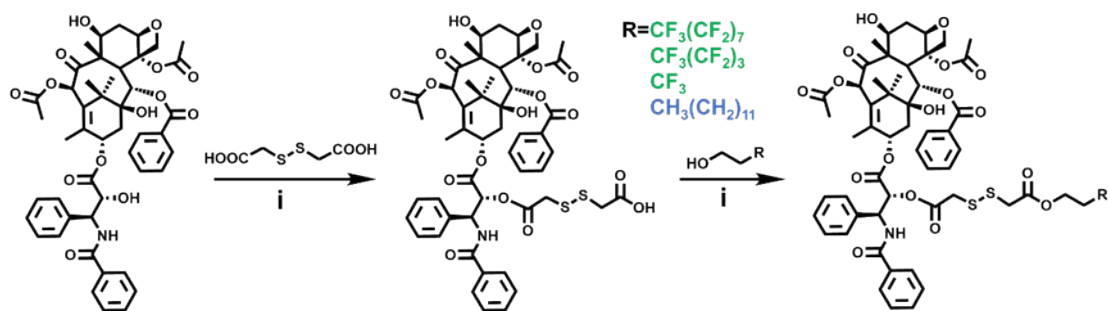


Fig. S1. The synthetic route of disulfide bond-bridged fluorinated/alkylated PTX prodrugs. i, EDC·HCl and DMAP at 25 °C.

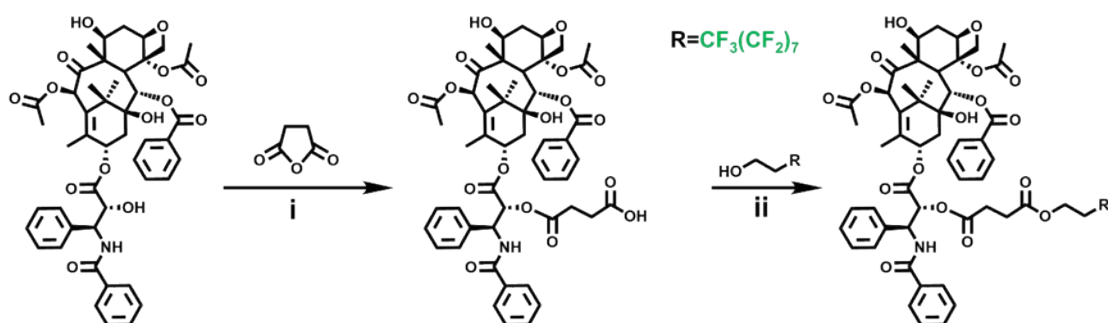


Fig. S2. The synthetic route of dicarbide bond-bridged fluorinated PTX prodrug PC-17F. i, DMAP and pyridine at 25 °C; ii, EDC·HCl and DMAP at 25 °C.

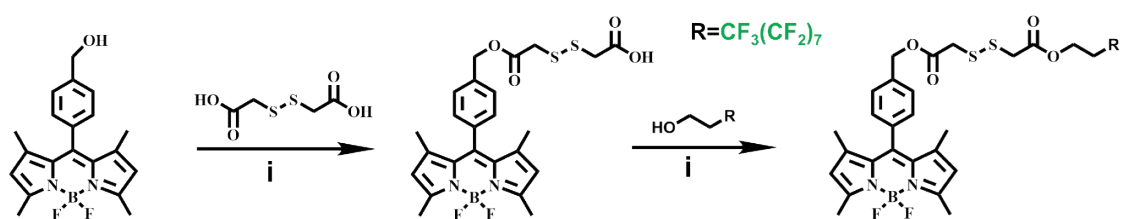


Fig. S3. The synthetic route of BDP-17F. i, EDC·HCl and DMAP at 25 °C.

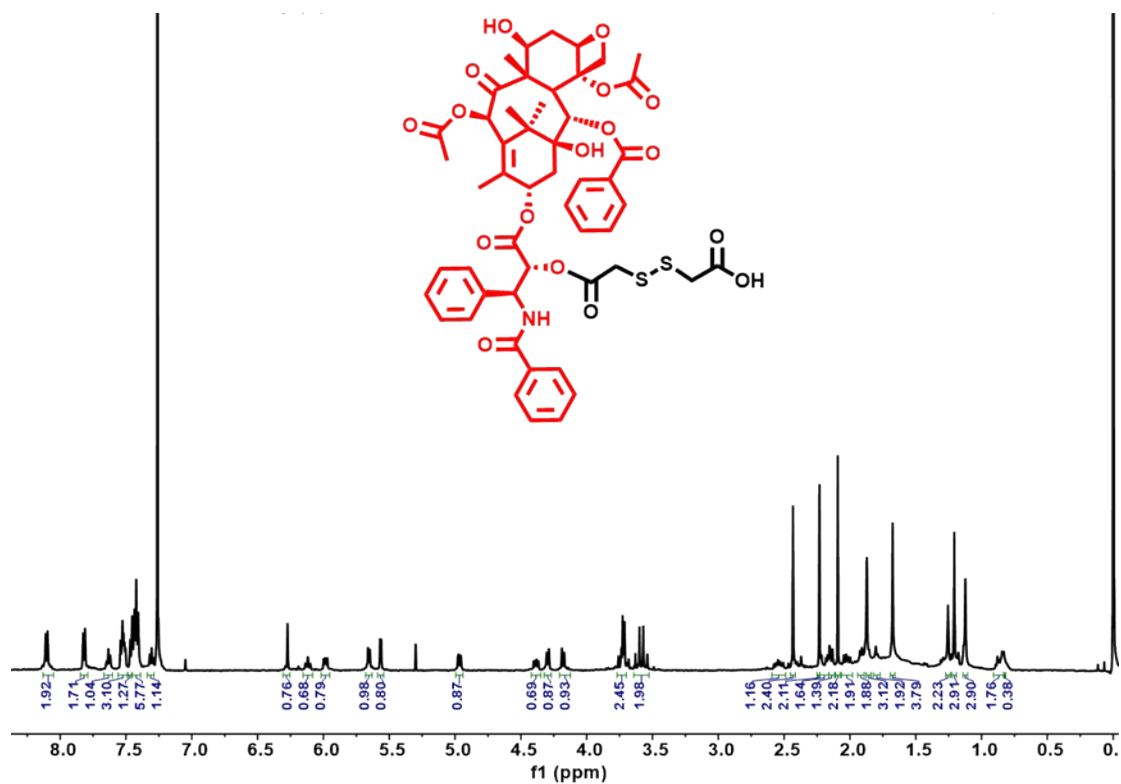


Fig. S4. ¹H NMR spectrum of PTX-SS-COOH in CDCl₃.

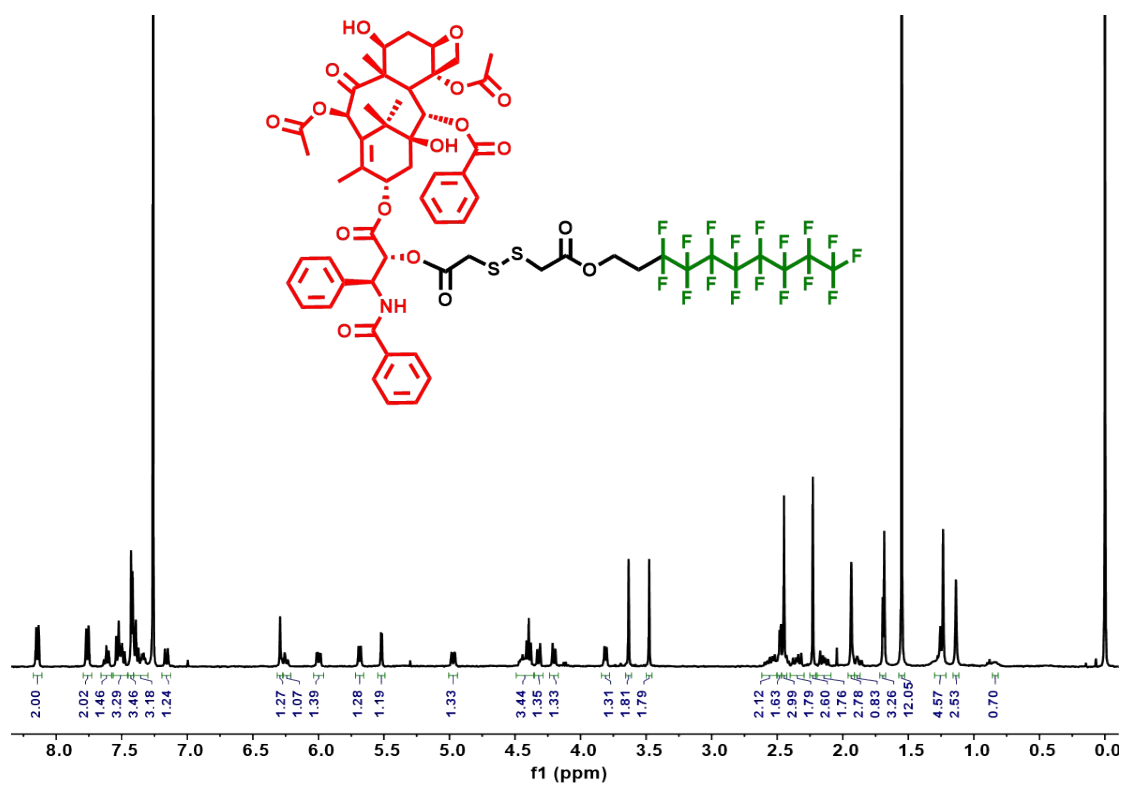


Fig. S5. ¹H NMR spectrum of PS-17F in CDCl₃.

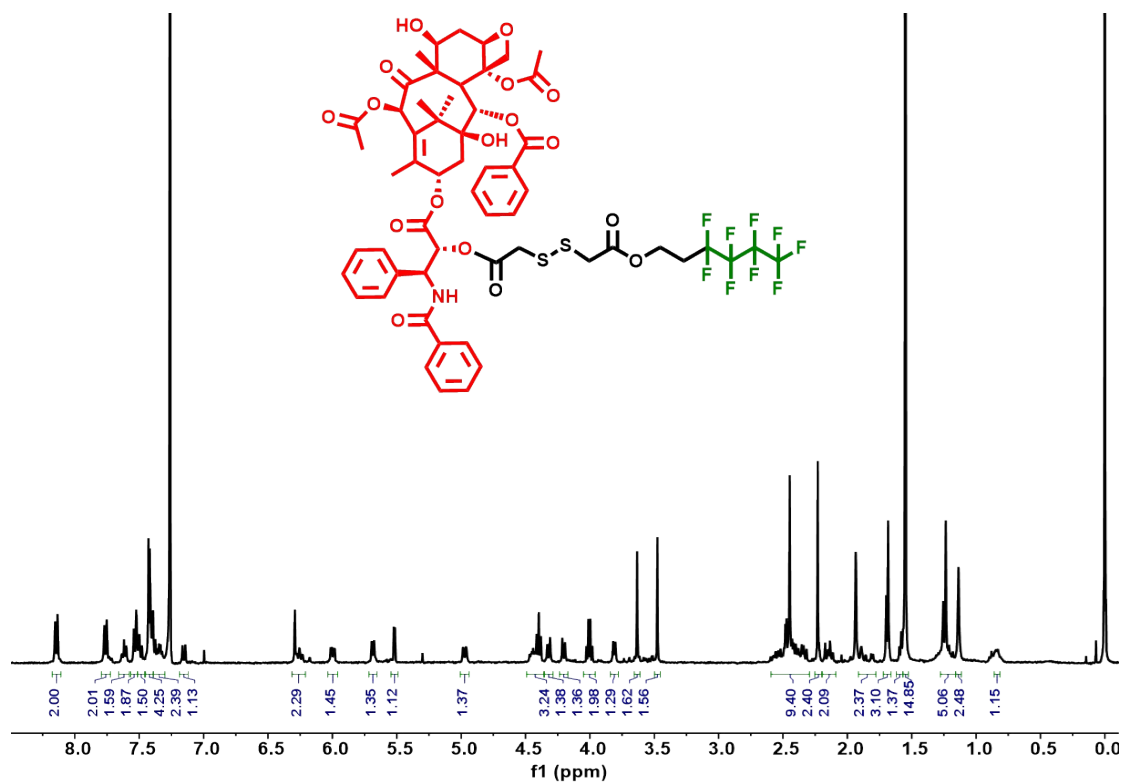


Fig. S6. ^1H NMR spectrum of PS-9F in CDCl_3 .

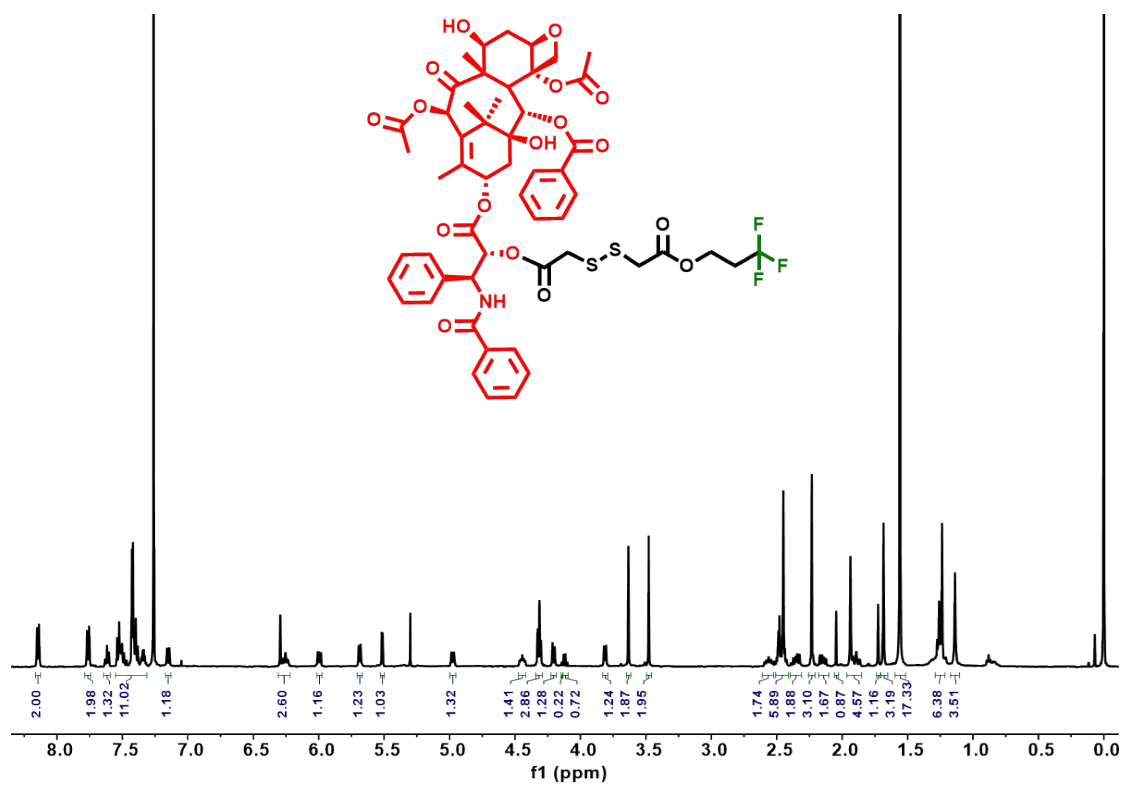


Fig. S7. ^1H NMR spectrum of PS-3F in CDCl_3 .

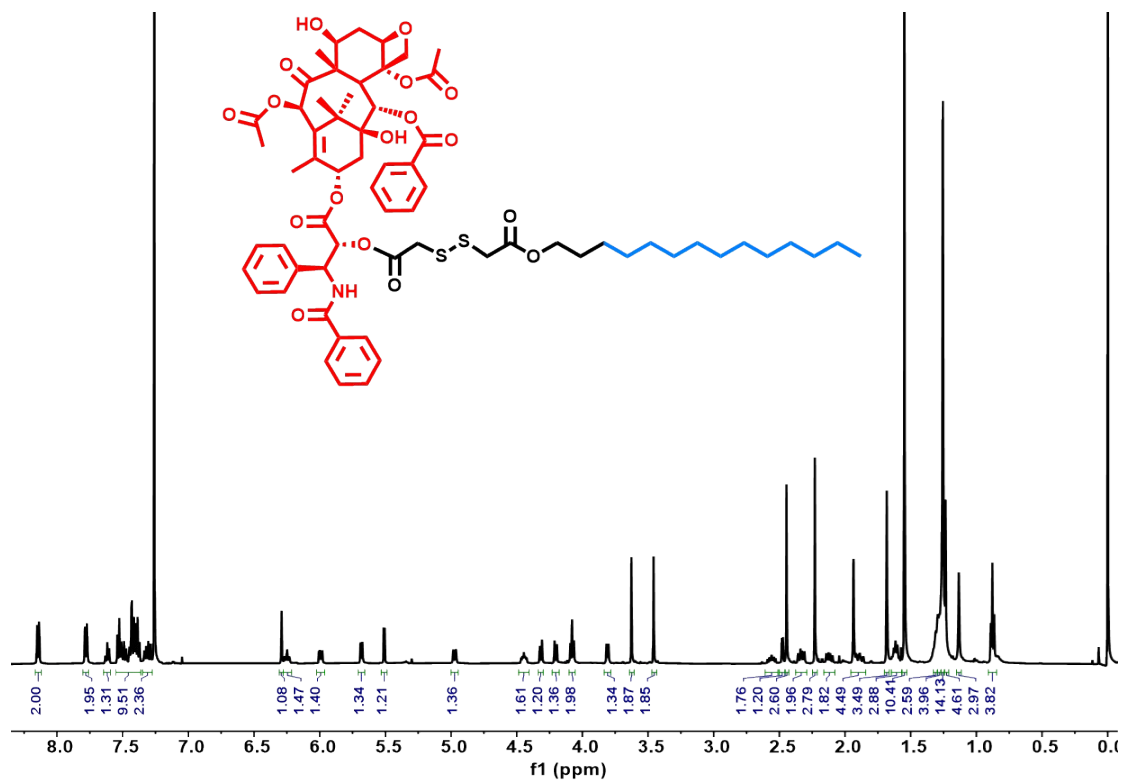


Fig. S8. ¹H NMR spectrum of PS-CH in CDCl₃.

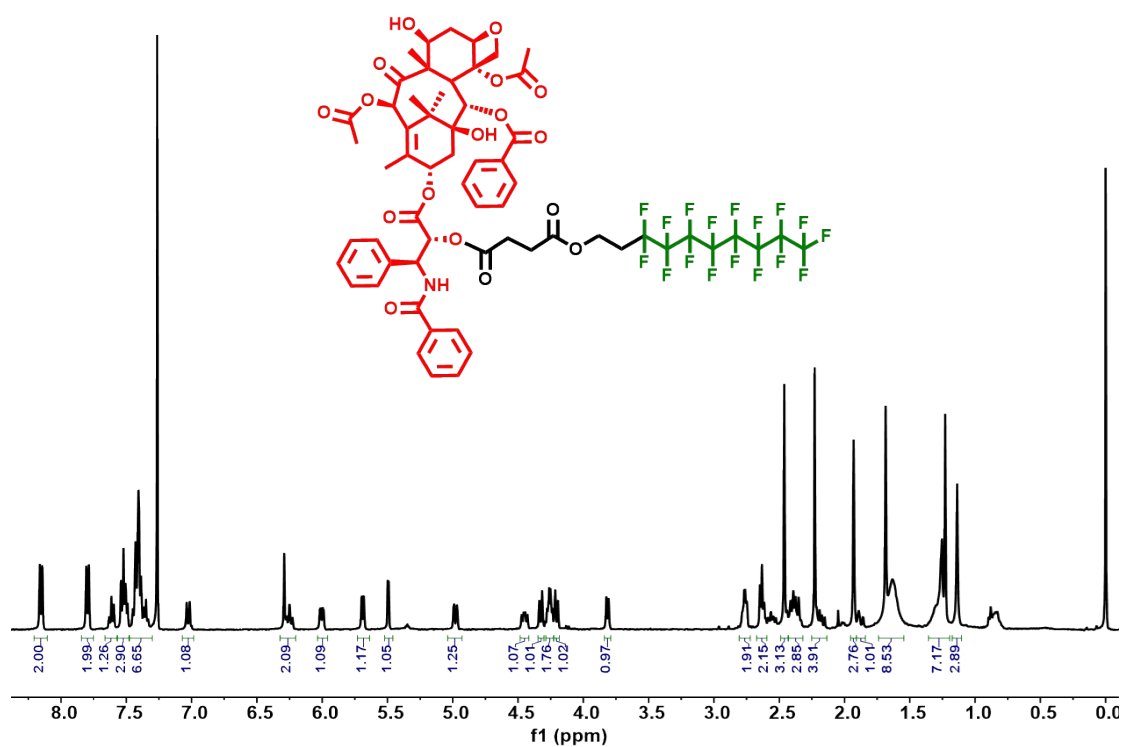


Fig. S9. ¹H NMR spectrum of PC-17F in CDCl₃.

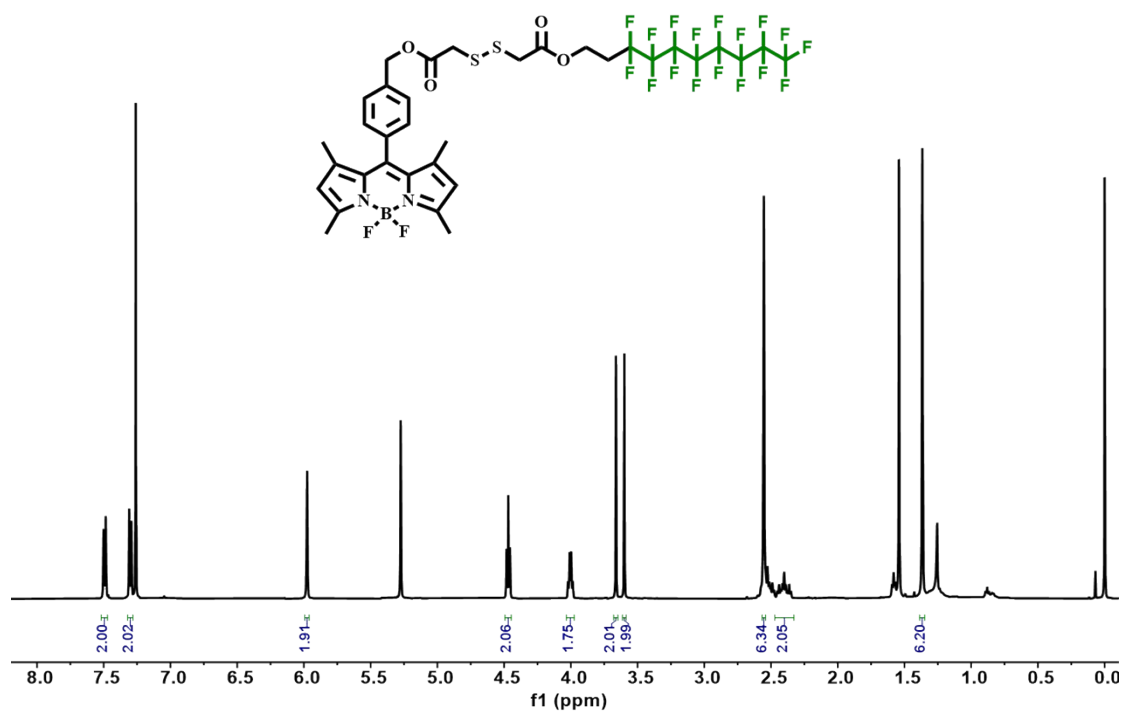


Fig. S10. ^1H NMR spectrum of BDP-17F in CDCl_3 .

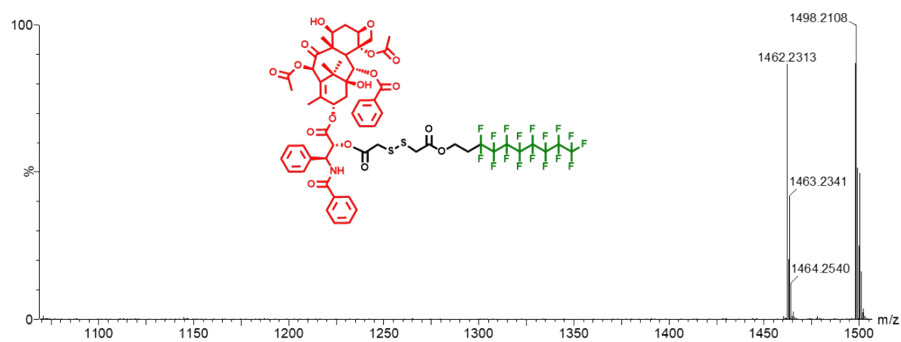


Fig. S11. ESI-TOF mass spectrum of PS-17F.

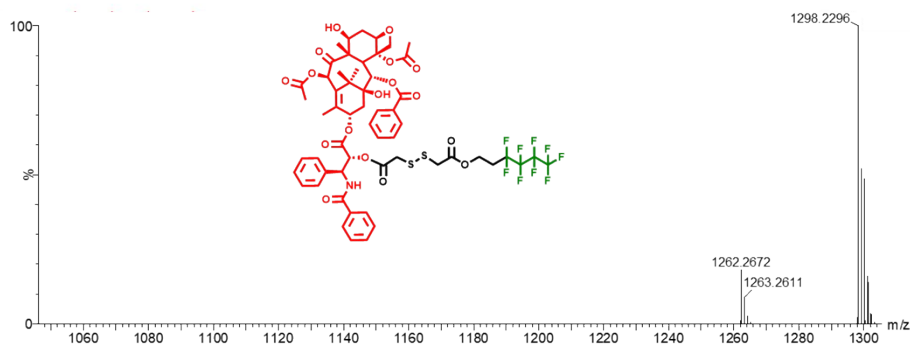


Fig. S12. ESI-TOF mass spectrum of PS-9F.

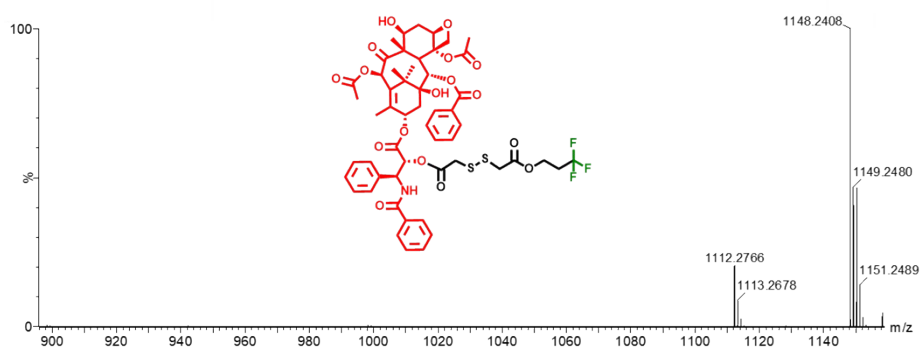


Fig. S13. ESI-TOF mass spectrum of PS-3F.

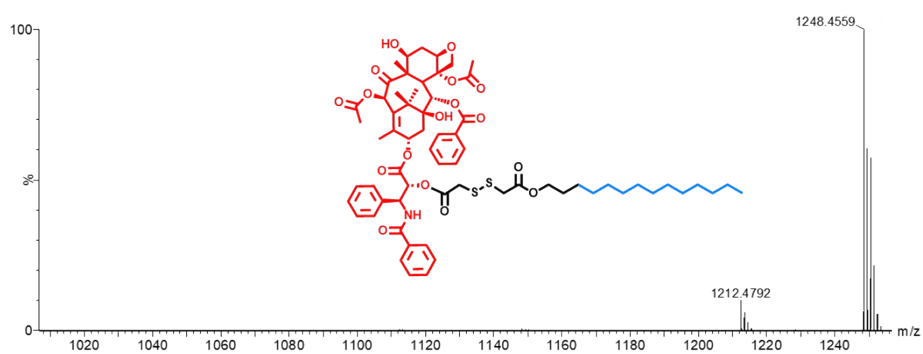


Fig. S14. ESI-TOF mass spectrum of PS-CH.

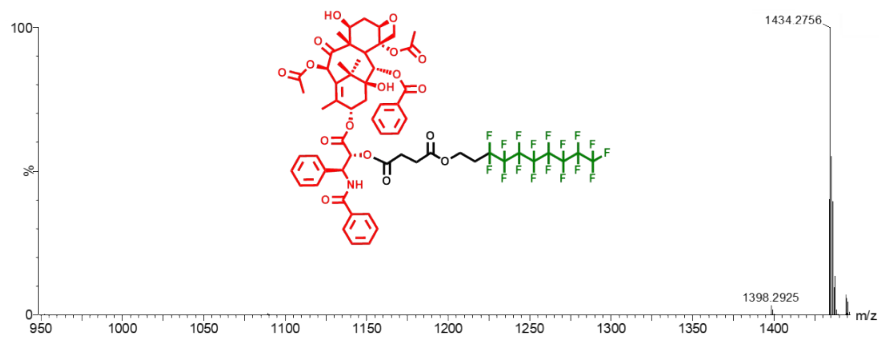


Fig. S15. ESI-TOF mass spectrum of PC-17F.

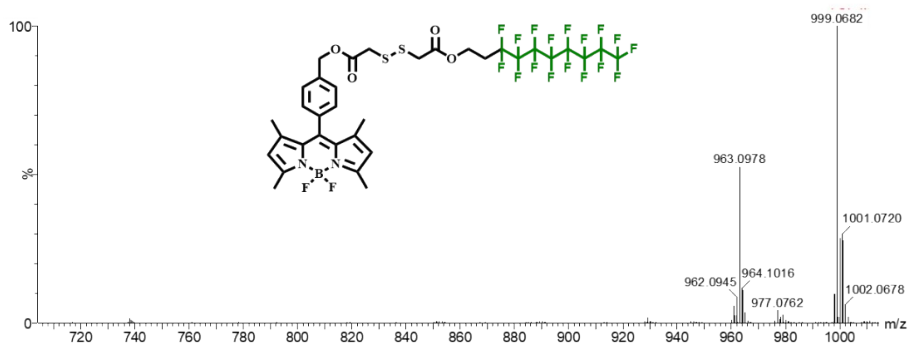


Fig. S16. ESI-TOF mass spectrum of BDP-17F.

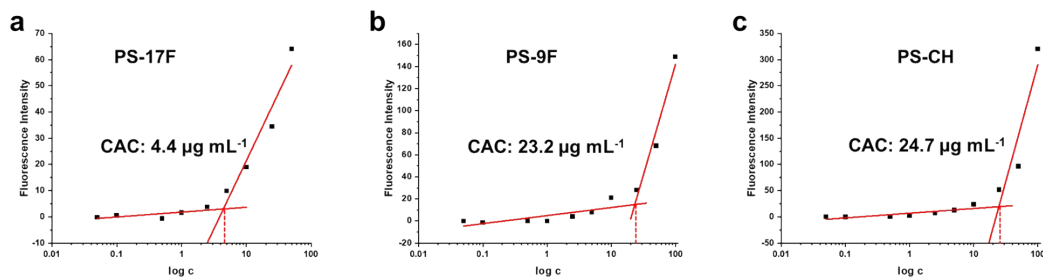


Fig. S17. The CAC of PS-17F (a), PS-9F (b) and PS-CH (c).

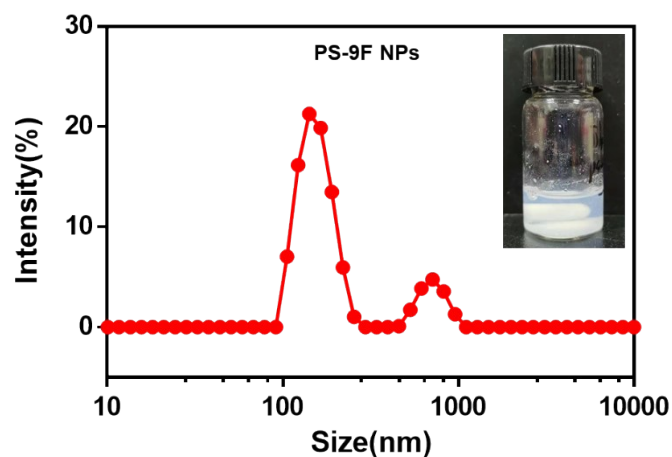


Fig. S18. The size distribution and picture of PS-9F NPs at the concentration of 0.34 mg mL^{-1} .

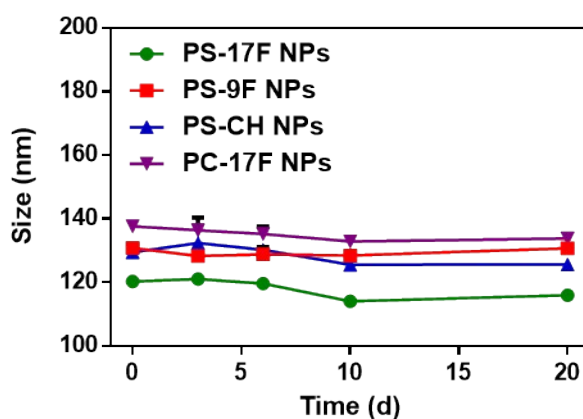


Fig. S19. The size of PS-17F NPs, PS-9F NPs, PS-CH NPs and PC-17F NPs after storage in water for 20 days.

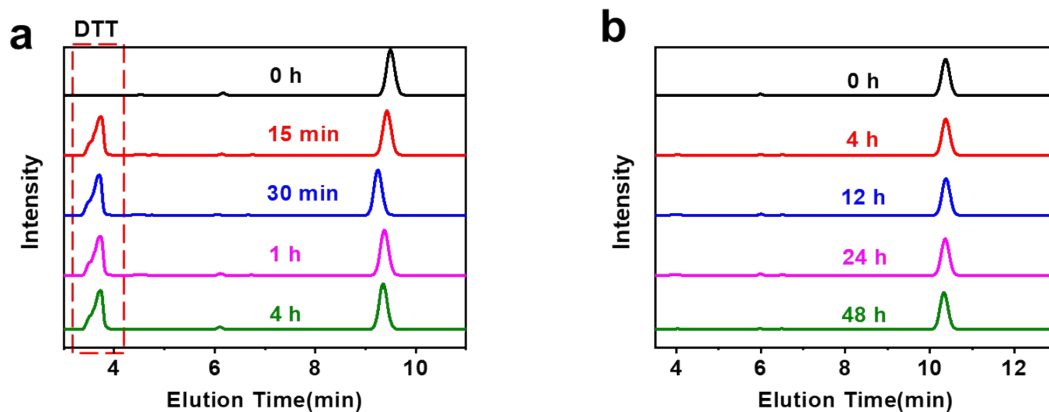


Fig. S20. The redox-responsive PTX release from PC-17F NPs upon being treated with 10 mM DTT (a) and 10 mM H₂O₂ (b).

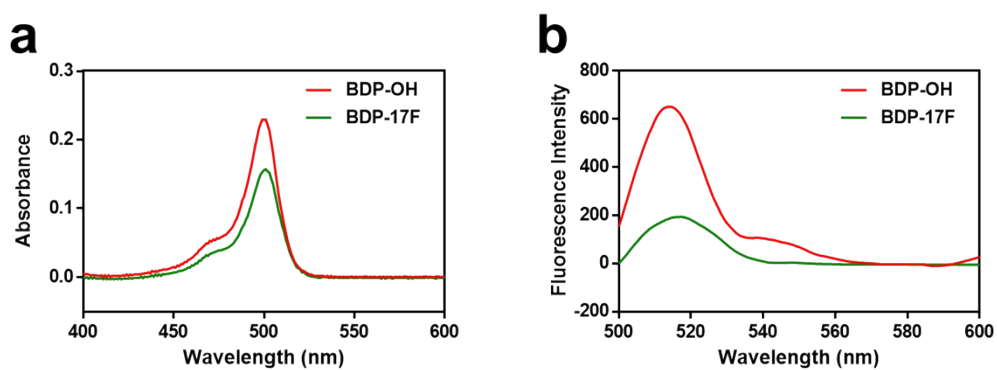


Fig. S21. UV-vis absorption spectra (a) and FL emission spectra (b) of BDP-OH and BDP-17F at equivalent BDP concentration of 2 μ M in DMF.

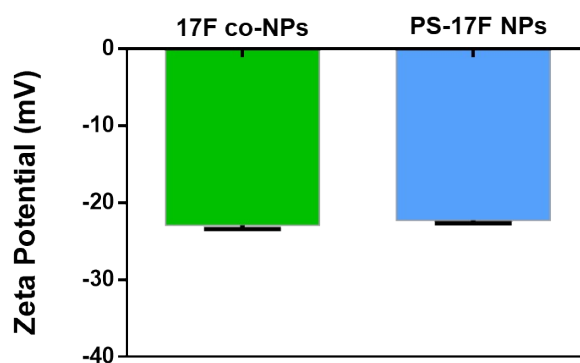


Fig. S22. ζ -potential of 17F co-NPs and PS-17F NPs.

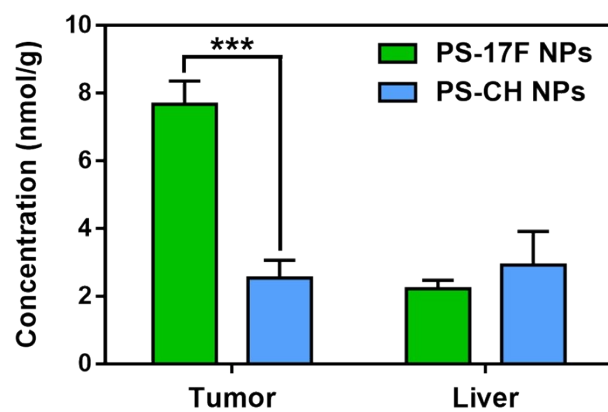


Fig. S23. Tumor accumulation of PS-17F NPs and PS-CH NPs (n = 3). *P < 0.05,

P < 0.01, and *P < 0.001.